Plant Cell Physiol. 48(6): 843–855 (2007)
doi:10.1093/pcp/pcm055, available online at www.pcp.oxfordjournals.org

Xyloglucan *Endo*-transglycosylase (XET) Functions in Gelatinous Layers of Tension Wood Fibers in Poplar—A Glimpse into the Mechanism of the Balancing Act of Trees

Nobuyuki Nishikubo [1,5,8], Tatsuya Awano [1,6,8], Alicja Banasiak [1,7], Veronica Bourquin [1], Farid Ibatullin [2], Ryo Funada [3], Harry Brumer [2], Tuula T. Teeri [2], Takahisa Hayashi [4], Björn Sundberg [1] and Ewa J. Mellerowicz [1,*]

[1] *Department of Forest Genetics and Plant Physiology, Umea Plant Science Center, SLU, S901 83 Umea, Sweden*
[2] *Department of Biotechnology, Royal Insitute of Technology (KTH), S-106 91 Stockholm, Sweden*
[3] *Faculty of Agriculture, Tokyo University of Agriculture and Technology, Fuchu-Tokyo 183-8509 Japan*
[4] *Research Institute for Sustainable Humanosphere, Kyoto University, Kyoto, 611-0011 Japan*

Tension wood is a specialized tissue of deciduous trees that functions in bending woody stems to optimize their position in space. Tension wood fibers that develop on one side of the stem have an increased potency to shrink compared with fibers on the opposite side, thus creating a bending moment. It is believed that the gelatinous (G) cell wall layer containing almost pure cellulose of tension wood fibers is pivotal to their shrinking. By analyzing saccharide composition and linkage in isolated G-layers of poplar, we found that they contain some matrix components in addition to cellulose, of which xyloglucan is the most abundant. Xyloglucan, xyloglucan *endo*-transglycosylase (XET) activity and xyloglucan *endo*-transglycosylase/hydrolase (*XTH*) gene products were detected in developing G-layers by labeling using CCRC-M1 monoclonal antibody, in situ incorporation of XXXG-SR and the polyclonal antibody to poplar *Ptt*XET16-34, respectively, indicating that xyloglucan is incorporated into the G-layer during its development. Moreover, several *XTH* transcripts were altered and were generally up-regulated in developing tension wood compared with normal wood. In mature G-fibers, *XTH* gene products were detected in the G-layers while the XET activity was evident in the adjacent S_2 wall layer. We propose that XET activity is essential for G-fiber shrinking by repairing xyloglucan cross-links between G- and S_2-layers and thus maintaining their contact. Surprisingly, *XTH* gene products and XET activity persisted in mature G-fibers for several years, suggesting that the enzyme functions after cell death repairing the cross-links as they are being broken during the shrinking process.

Keywords: Gravity responses — *Populus* — Reaction wood — Secondary wall — Wood formation — Xylogenesis.

Abbreviations: ADF6, actin depolymerizing factor 6; CW, compression wood; DMSO, dimethylsulfoxide; elF4A-8, eukaryotic initiation factor 4A-8; EST, expressed sequence tag; FITC, fluorescein isothiocyanate; G, gelatinous; NW, normal wood; OW, opposite wood; TW, tension wood; UBQ4, polyubiquitin 4; XET, xyloglucan *endo*-transglycosylase; XG, xyloglucan; XTH16, xyloglucan *endo*-transglycosylase/hydrolase of family GH16; XXXG-SR, sulforhodamine-labeled xylogluco-oligosaccharide.

The nucleotide sequences reported in this paper have been submitted to GenBank under the following accession numbers: *XTH16-34*, AF515607; *XTH16-26*, EF194046; *XTH16-35*, EF151160; *XTH16-36*, EF194050; *XTH16-6*, EF194049; *XTH16-21*, EF194058; *XTH16-30*, EF194057; *XTH16-17*, EF194056; *XTH16-39*, EF194055; *XTH16-14*, EF194054; *XTH16-3*, EF194053; *XTH16-27*, EF194052; *XTH16-1*, EF194048; *XTH16-38*, EF194047; *XTH16-25*, EF194051; *XTH16-29*, EF194045.

Introduction

Tree growth habit involves the formation of thick stems elevating a large photosynthetic crown. This structure poses a challenge for how to maintain it in balance in the gravitational field and keep the heavy branches with foliage leaves optimally exposed to the light. While herbaceous plants maintain their position in space by the asymmetric growth of the shoot elongation zone leading to the bending of the stem by gravitropic and phototropic growth, trees require a different strategy that allows them to bend their stems in the non-elongating zone where thick secondary growth is present.

Conifers and angiosperms evolved different strategies to achieve the bending of the stem with secondary growth. Both these strategies involve the formation of the reaction wood asymmetrically on one side of the stem.

[5]Present address: RIKEN Plant Science Center, 1-7-22 Suehiro-cho Tsurumi-ku, Yokohama, Kanagawa, 230-0045 Japan.
[6]Present address: Laboratory of Tree Cell Biology, Division of Forest and Biomaterials Science, Graduate School of Agriculture, Kyoto University, Kyoto, 606-8502 Japan.
[7]Present address: Institute of Plant Biology, University of Wroclaw, Kanonia 6/8, 50-328, Wroclaw, Poland.
[8]These authors contributed equally to this work.
*Corresponding author: E-mail, ewa.mellerowicz@genfys.slu.se; Fax, +46-90-786-8165.

Conifers produce the compression wood (CW) on the side of the stem that needs to elongate more compared with the opposite side, while angiosperms produce the tension wood (TW) on the side of the stem that needs to shrink relative to the other side. In a typical TW, a specialized gelatinous (G) wall layer is formed during the final stage of fiber differentiation, partially replacing S_3-, S_2- and, in some species, also S_1-layers. Many properties of TW and CW differ from normal wood (NW) in opposite ways. While the typical TW is less lignified, and has more longitudinally oriented cellulose microfibrils, higher cellulose crystallinity and higher cellulose content, the CW contains more lignin and has a flatter microfibril angle, less crystalline cellulose and lower cellulose content than NW (reviewed in Timmel 1986, Pilate et al. 2004). It is thought that the structural differences between the reaction wood and the wood on the opposite side (so-called opposite wood, OW) induce different residual growth stresses of both sides of the stem, resulting in a bending moment (Fournier et al. 1994, Bamber 2001, Almeras et al. 2005, Clair et al. 2006a).

The mechanism of growth stress generation and its modification by either type of reaction wood is not quite clear. It is thought that the newly produced cells have the inherent tendency to shrink longitudinally during maturation but, since they are held extended by the older xylem cells located centripetally in the stem, a tensile stress develops in the outer cell layers of the stem (Hejnowicz, 1997, Plomion et al. 2001). Strain measurement on the stem surface in hardwood species indicated that the TW has up to 20 times higher tensile stress than the OW or NW (Fournier et al. 1994, Clair et al. 2006a, Clair et al. 2006b, Clair et al. 2006c). Thus, when transverse cuts are made at the wood surface, the tensile stress is released, and the isolated TW shrinks. It has been shown recently that the stress relaxation observed macroscopically on the stem surface corresponds to that observed at the nano level in cellulose microfibrils of the G-layer (Clair et al. 2006b). The microfibril shrinkage was observed as a decrease of the cellulose lattice spacing, when the tensile strain was released in TW. These are the first direct observations confirming a long-suspected mechanical role for the G-layer cellulose microfibrils in stem re-orientation (Bamber 2001, Yamamoto et al. 2005).

The proposed role for the G-layer in stem bending necessitates that it be mechanically fastened to the outer cell wall layers (S_1, S_2 or S_3, if present), so that the entire TW fiber will shrink upon G-layer microfibril shrinkage. The ultrastructure of the cell wall in TW fibers revealed that the cellulose microfibril angle changes between the G-layer and adjacent S-layer from axial to inclined, so that the transition zone between these layers has a low density of cellulose microfibrils (Araki et al. 1982, Prodhan et al. 1995). This creates a mechanically weakened area, where the attachment between layers must be provided by means other than cellulose cell wall components, such as cross-linking glycans, extensin or pectins. However, the information on the chemical composition of the G-layers does not provide many clues as to how the attachment could be formed because the layers were found to contain almost pure cellulose (Norberg and Meier 1966).

Here we provide the evidence that xyloglucan (XG) is a component of G-layers of TW poplar fibers. We also demonstrate that glycoside hydrolase family GH16 xyloglucan *endo*-transglycosylase/hydrolase (*XTH16*) gene products (Geisler-Lee et al. 2006) and xyloglucan *endo*-transglycosylase (XET; EC 2.4.1.207) activity are found in the TW fibers during their differentiation and are localized in the G-layer. In addition, we show that transcript levels of several different *XTH16* genes are altered between developing TW and NW, and are generally up-regulated in TW during S_1/S_2- and G-layer formation. In mature fibers, the protein is still detectable in the G-layer while the activity is seen in the adjacent S_2 wall layer for at least 3 years, long after completion of the differentiation process. These observations suggest a role for particular enzyme isoforms in readjusting cross-linking glycans of the G-layer needed for G-fiber action, and show, for the first time, that these processes might extend beyond the lifespan of TW fibers.

Results

Carbohydrate components of the G-layer

Previous studies established that G-layers of poplar TW contained almost pure cellulose with a small amount of other, not well defined carbohydrates (Norberg and Meier 1966). To determine the nature of the G-layer carbohydrates, we isolated mature G-layers by sonicating cross-sections of TW from a field-grown tree and determined their neutral sugar composition. The isolated G-layers were free of contaminants from other cell wall layers, as was verified by microscopic inspection (Fig. 1). Pure G-layers were directly hydrolyzed to monosaccharides with sulfuric acid and assayed by gas chromatography (Borchardt and Piper 1970). In addition to glucose (88.8 mol%), the analysis detected >5 mol% of xylose and >1 mol% of fucose, galactose and mannose (Table 1). Rhamnose and arabinose were also detected. This indicates that the G-layer contains >10 mol% of non-cellulosic carbohydrates.

In order to determine the nature of the non-cellulosic carbohydrates, the isolated G-layers were solubilized in dimethylsulfoxide (DMSO) containing tetrabutylammonium fluoride (Lu and Ralph 2003) and subjected to methylation analysis (Hakomori 1964). The most abundant component beside 4-glucose was 4,6-glucose (9 mol%)

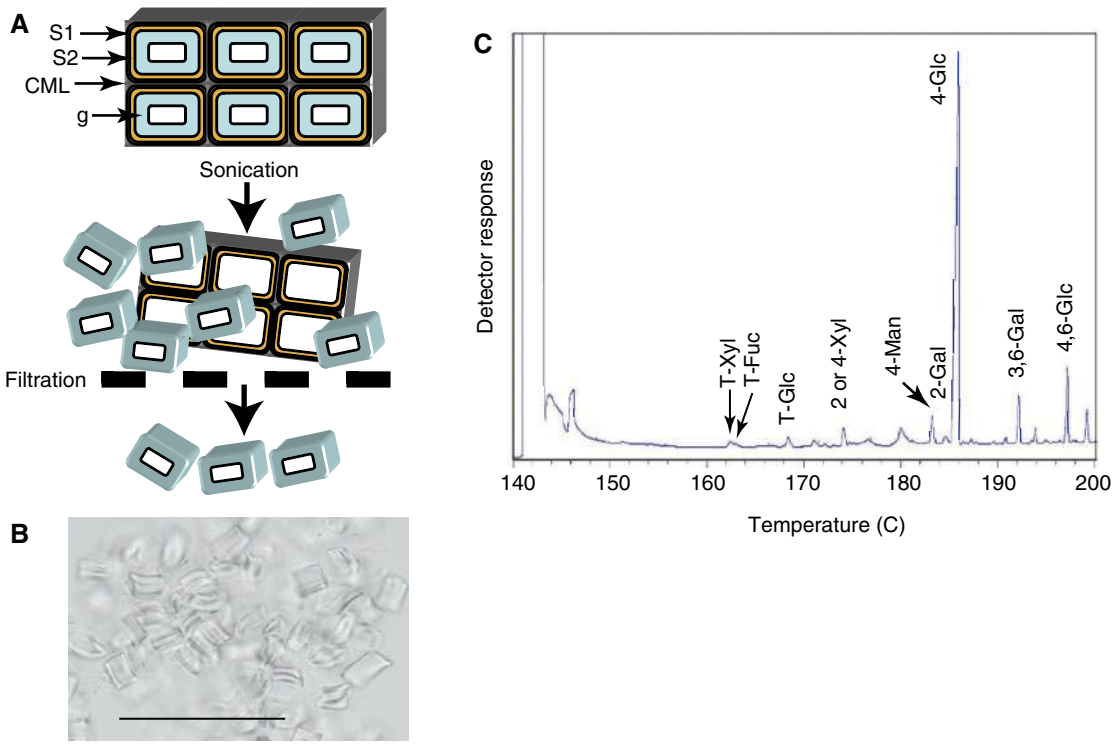

Fig. 1 Carbohydrate linkage analysis of the isolated G-layers. (A) Diagram of successive steps of the G-layer isolation procedure by ultrasonic treatment of transverse sections of mature TW. Due to their weak attachment to S2 wall layers, the G-layers are removed from the sections by sonication treatment. CML, compound middle lamella; g, G-layer, S1, S2, successive secondary wall layers. (B) Micrograph of the isolated G-layers showing a lack of contamination from other cell wall layers that remain intact after the treatment. Bar = 100 µm. (C) Methylation analysis of the monosaccharides contained in the G-layers, showing the presence of the 4,6-glucose diagnostic for XG.

Table 1 Neutral sugar composition of the isolated G-layers of *P. alba*

Relative amount of neutral monosaccharide (mol%)						
Rhamnose	Fucose	Arabinose	Xylose	Mannose	Galactose	Glucose
0.6	1.3	0.7	5.6	2.1	1.1	88.6

which indicates that the xyloglucan is one of the major non-cellulosic components of the G-layer (Fig. 1, Table 2). T-Fucose, T-xylose and 2-galactose residues also indicate the presence of fucosylated xyloglucan in the G-layer. In addition, there was 5.5 mol% of 3,6-galactose, indicating the presence of arabinogalactan II, and 2.2 mol% of 4-mannose, indicating the presence of β-1,4-mannan. The presence of arabinogalactan II has been indicated previously by staining of the G-layers with the JIM14 monoclonal antibody, which is consistent with a strong up-regulation of FLA12-like proteins during TW formation (Lafarguette et al. 2004, Andersson-Gunerås et al. 2006). However, judging from the amount of xylose and the amount of 4,6-linked glucose, the XG is by far the main non-cellulosic component of the G-layers in poplar.

Localization of xyloglucan in tension wood

Chemical analysis of isolated G-layers indicated the presence of XG in these cell wall layers. To confirm this conjecture and to determine the distribution of XG within the cell wall layers of G-fibers, the CCRC-M1 monoclonal antibody that binds the fucose side chain of XG (Puhlmann et al. 1994) was used to label the developing TW in situ. In developing NW, the prominent label is found in the primary walls of all cell types at the primary walled stage (Bourquin et al. 2002). Prominent CCRC-M1 labeling

was also found in developing G-fibers at the primary walled stage (not shown). During secondary wall deposition in G-fibers, the CCRC-M1 label was evident in the currently formed layer and was most prominent in the developing G-layer (Fig. 2). Some signal was also evident in the compound middle lamella (Fig. 2A, D, F), which is the location of XG in NW fibers (Bourquin et al. 2002). In contrast to the uniform labeling of the primary cell wall, the label in the G-layer was uneven, patchy or more obvious at the layer outer boundary. In the mature TW fibers, CCRC-M1 labeled only the compound middle lamella (Fig. 2 B, E). This signal was not due to the autofluorescence of lignin, as it was not detected in the section where the CCRC-M1 antibody was omitted (Fig. 2C).

Table 2 Glycosyl linkages of carbohydrates in the isolated G-layers of *P. alba*

Glycosyl	Linkage	Fraction (mol%)	Potential components
Xylosyl	Terminal	1.2	Xyloglucan
	2- or 4-linked	3.0	Xyloglucan, xylan
Fucosyl	Terminal	0.5	Xyloglucan
Glucosyl	Terminal	1.9	Cellulose, xyloglucan, glucomannan
	4-linked	75.6	Cellulose, xyloglucan, glucomannan
	4,6-linked	9.0	Xyloglucan
Galactosyl	2-linked	0.9	Xyloglucan
	3,6-linked	5.5	Arabinogalactan
Mannosyl	4-linked	2.2	Glucomannan

This transient presence of CCRC-M1 label in the developing G-layer, which nevertheless contains XG at maturity, as determined by the chemical analysis of the isolated mature G-layers, suggests that XG is accessible to the antibody only during its incorporation into the layer, later being masked by some other interacting component(s).

Developing G-layers specifically incorporate xylogluco-oligosaccharides

To confirm that developing G-fibers incorporate XG into the G-layers, we proceeded with in situ analysis of the incorporation of the sulforhodamine-labeled xylogluco-oligosaccharide in developing TW. XG is normally incorporated into the cell wall by the action of the cell wall resident xyloglucan:xyloglucosyl transferase (XET; EC 2.4.1.207). Therefore, freshly sectioned TW was incubated with the sulforhodamine-labeled xylogluco-oligosaccharide XXXG-SR for 30 min, after which time

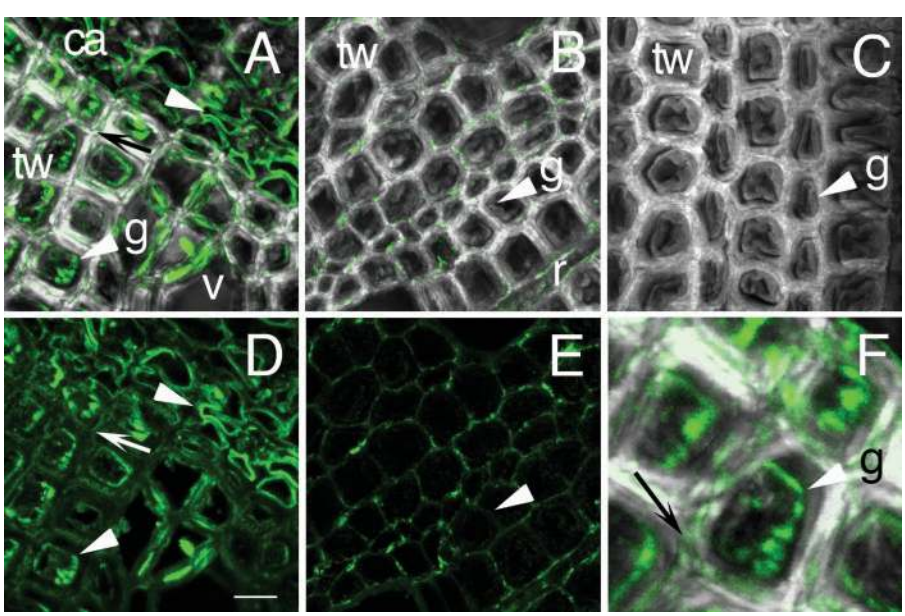

Fig. 2 Localization of XG with the monoclonal antibody CCRC-M1 in the developing G-fibers (A, D) and in mature G-fibers (B, E) from *P. tremula* grown in the field. Top row and F: the CCRC-M1 signal (green) superimposed on the transmitted light image; D and E show the signal only. The negative control labeled with the secondary antibodies only (C) shows no signal. In the young G-fibers pictured in A and D, and in the higher magnification in F, the label is evident in the G-layer (g) with a patchy appearance compared with a uniform labeling of the primary cell wall of the cambial cells (ca). Some label is found in the compound middle lamella (arrows). In the mature fibers (B, E), the label is found only in the compound middle lamella while the G-layer (arrowhead) is free of signal. Bar = 10 µm (A–E).

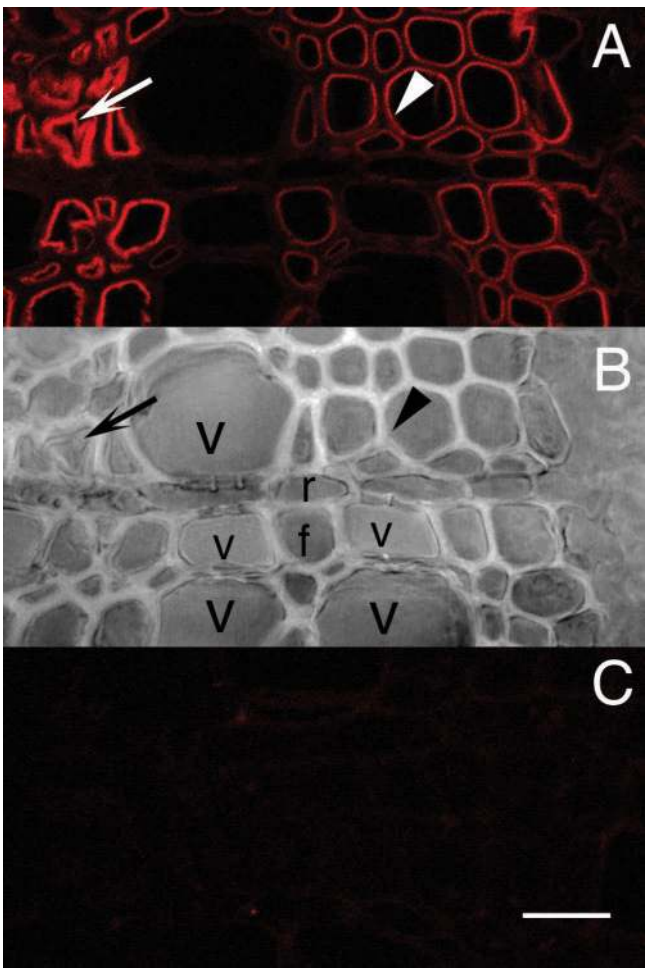

Fig. 3 In situ XET activity in developing G-fibers of a greenhouse-grown tree demonstrated by incorporation of XXXG-SR (A), the corresponding transmitted light image (B) and the negative control with boiled tissue (C). In the young developing G-fibers pictured here, the cell wall shows XXXG-SR incorporation throughout development (arrowhead). Later, only the G-layer is labeled (arrow). The walls of the ray cells (r) and vessel elements (v) do not show any activity. Cambium is to the right (out of focus); f, fiber; Bar = 20 μm.

the non-incorporated substrate was washed away and the label that was incorporated into cell walls was observed with a confocal laser microscope (Vissenberg et al. 2000, Bourquin et al. 2002). In developing TW, XXXG-SR was incorporated into a currently developing wall layer, but most intensely in the developing G-layers (Fig. 3). Other adjacent cell types (ray parenchyma cells and vessel elements) did not show XXXG-SR incorporation into the cell wall during this stage of development, although NW fibers do incorporate xylogluco-oligosaccharides at the early stage of secondary wall formation (Bourquin et al. 2002). Thus, only G-fibers have a continuous ability to incorporate xylogluco-oligosaccharides during their differentiation, including secondary wall development and, in particular, G-layer formation, indicating the presence of XET activity and of the donor XG in the developing G-layers.

G-fibers show long-lived XET activity

To investigate the fate of XET activity in mature G-fibers, we tested the successive growth rings of trees growing in the field. Samples were collected at the end of the latewood formation period when the secondary wall was still being developed because at this developmental stage, we could better discern the cell wall layers since they were thicker than in the greenhouse-grown trees. In the TW of the current growth increment, the site of XET activity was similar to that observed in the greenhouse-grown trees, i.e. it was evident in a layer being currently formed, with most prominent incorporation into the developing G-layers (Fig. 4A, B, D, E). The incorporation of XXXG-SR shifted during fiber maturation from the G-layer to the S_2-layer. In mature fibers 1–4 years old, the label was uniquely incorporated into the secondary wall layers immediately adjacent to the G-layer (Fig. 4H, I, K, L). This could be seen when comparing the G-fibers with contrasting thickness of the secondary wall layers outside the G-layer in earlywood (Fig. 4H, K) and latewood (Fig. 4I, L). The normal wood fibers without the G-layer did not show any XET activity (Fig. 4G, J). Thus, XET activity is present specifically in the G-fibers, first in the G-layer, and then in the S_2-layer where it can persist for several years.

XTH gene products are localized in the developing and mature G-layers

To confirm the presence of the active XET enzyme in the G-fibers, we used a polyclonal antibody raised against recombinant *Ptt*XET16-34, previously named *Ptt*XET16A (Bourquin et al. 2002, Johansson et al. 2004, Kallas et al. 2005), for labeling of tissue sections. The three-dimensional structure of this enzyme has recently been solved (Johansson et al. 2004), and detailed bioinformatic analysis of XET-like proteins in glycosyl hydrolase family 16 has been performed (Geisler-Lee et al. 2006, Baumann et al. 2007). Due to a high degree of sequence similarity (http://www.cazy.org), it is expected that several isozymes are labeled with this antibody. In NW, the antibody binds cell walls in all cells at the primary walled stage, and the cell walls of developing fibers at the early secondary walled stage (Bourquin et al. 2002). In developing TW, we found in addition to the signals described above a prominent labeling of the G-layers (Fig. 5). Both developing and mature G-layers were prominently labeled. When the G-layer was fully developed, the signal was more concentrated in the outer zone of the G-layer close to the lignified S_2-layer (Fig. 5E).

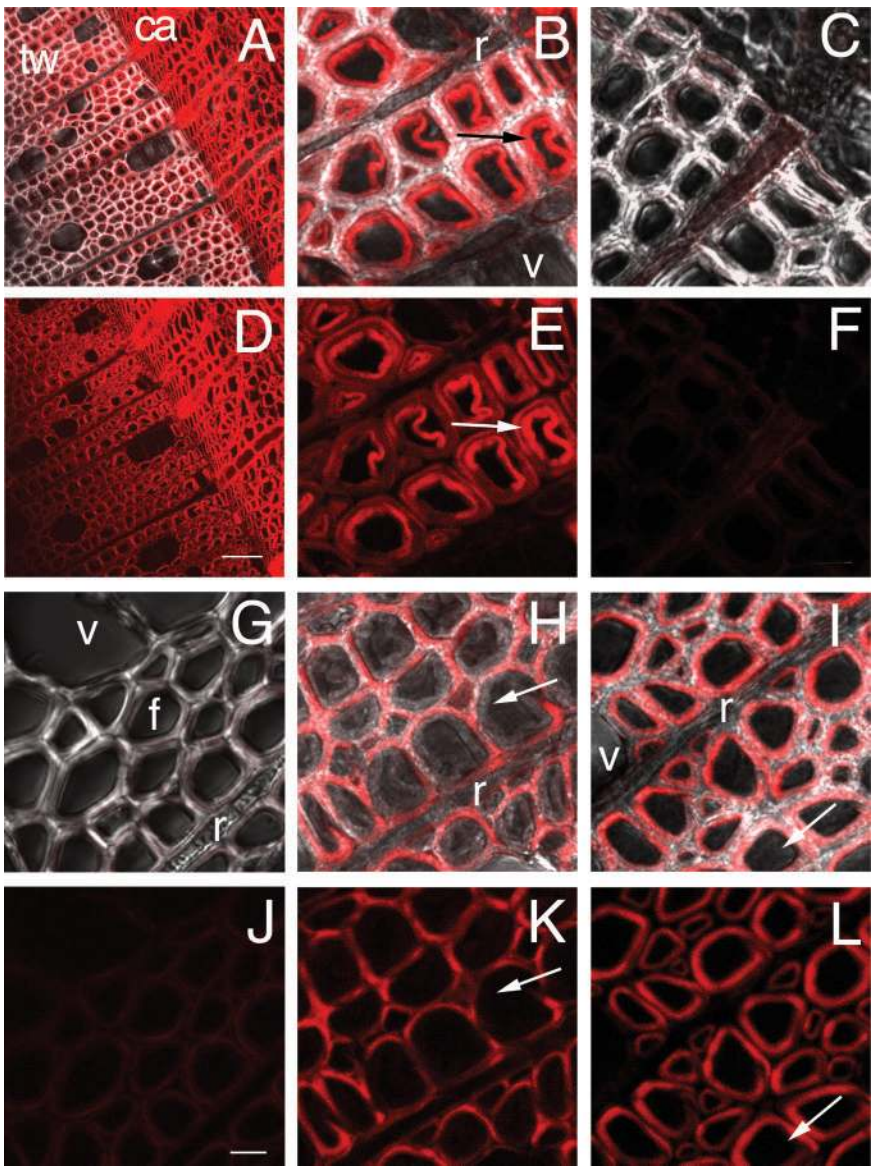

Fig. 4 In situ XET activity in the wood of a field-grown *P. tremula* demonstrated by incorporation of XXXG-SR (red signal). The top row of paired images shows the signal superimposed on the transmitted light image; the bottom row shows the signal only. (A–F) Developing G-fibers. The sample was collected at the end of cambial activity when secondary wall was developing but the radial expansion was complete. (B, E) Close-up of developing G-fibers; note the prominent XET activity signal from the developing G-layer (arrow). (C, F) Negative control boiled before the activity assay. (G–L) The fourth ring (=4-year-old wood) with normal wood (G, J), the early wood TW (H K) and late wood TW (I, L). The signal is always right outside the G-layer, indicated by an arrow, regardless of the thickness of the S_1- and S_2-layers. Note the lack of activity in vessels and rays. Bar = 50 µm for A and D, and 10 µm for the remaining panels. Ca, cambium; tw, TW; f, fiber; v, vessel; r, ray.

To determine if the enzyme was permanently incorporated into the fiber G-layer or if it was present only in the developing and recently formed fibers, we examined the TW of the outdoor-grown poplar trees that were several years old. Samples containing three annual growth rings were obtained and analyzed with *Ptt*XET16A antibody. The signal, distinct from the signal of the pre-immune serum, was found in all three growth rings (Fig. 6). It was most intense in the TW formed in the current year (year 1) compared with the TW formed 2 or 3 years before, and it was found specifically in G-layers. In contrast, normal fibers were never observed labeled with the *Ptt*XET16A antibody past the early differentiation stage, as also noted by Bourquin et al. (2002).

Several GH16 XTH genes are up-regulated during TW formation

To determine which genes could be responsible for the XET activity found in G-fibers, we first surveyed the available transcriptomics data for poplar. Previous transcriptomic analyses in poplar using expressed sequence tag (EST) frequency showed six genes among a total of 41 *XTH* genes found in the poplar genome with transcripts in the developing TW (Geisler-Lee et al. 2006). These included *XTH16-35* with five transcripts, *XTH16-38* with three transcripts and the remaining *XTH16-3*, *XTH16-27*, *XTH16-30* and *XTH16-34* with one transcript each. Analysis of *XTH* gene expression using cDNA microarrays (Andersson-Gunneråas et al. 2006) revealed changes in a few

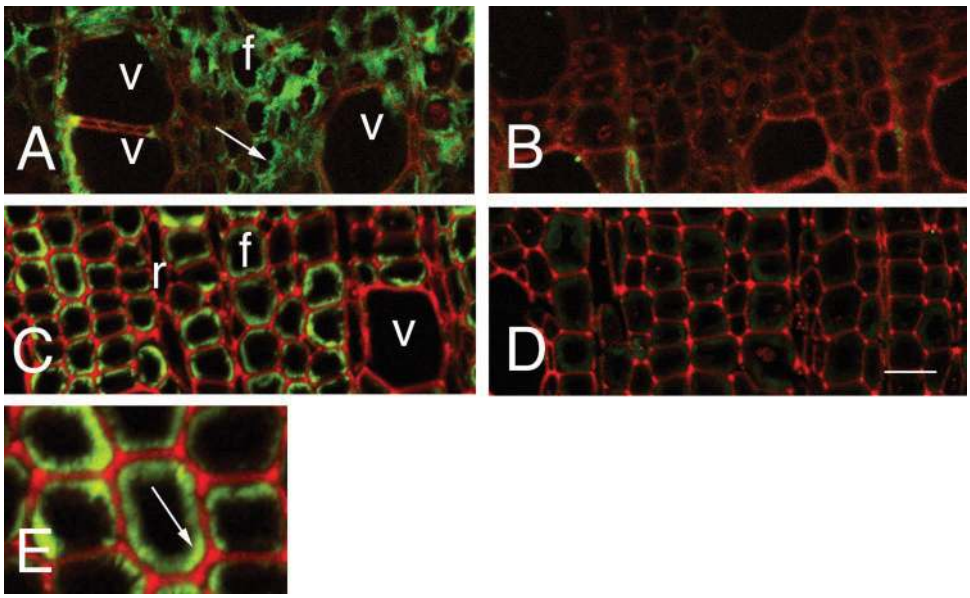

Fig. 5 Immunolocalization of XTH proteins in TW recognized by anti-*Ptt*XET16-34 polyclonal antibody XET16A (A and C) and the negative control signal from the pre-immune serum (B and D). Green indicates the signal from the antibody; red is the autofluorescence of cell walls. A and B show developing TW fibers; cambium is to the top (not in the picture). XTH signal can be seen in the developing G-layer (arrow). C and D show fully developed TW fibers with lignified compound middle lamella, S_1- and S_2-layers as marked by intense autofluorescence. XTH signals are abundant in G-layers (arrow). (E) A magnified image of TW fibers from (C) showing a high intensity XTH signal in the G-layer (arrow), in pariticular close to the lignified (red) S_2-layer. f, fiber; v, vessel; r, ray. Bar = 20 μm.

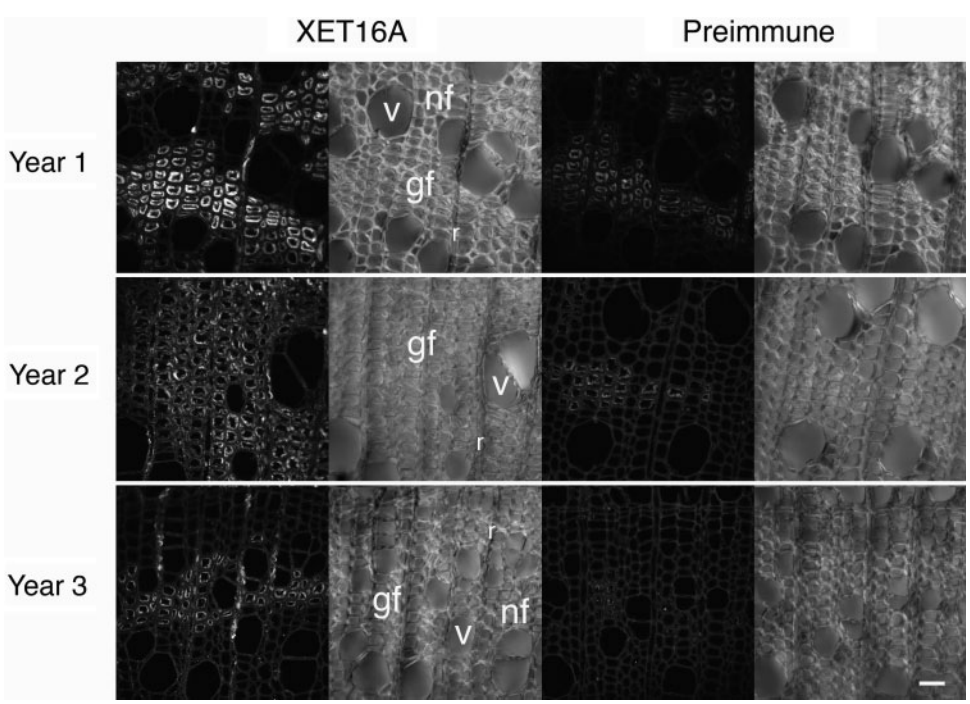

Fig. 6 Localization of XTH proteins in successive growth rings of TW in the outdoor-grown poplar (*P. alba*) using anti-*Ptt*XET1616-34 antibody XET16A. The pre-immune serum is used for labeling of the background signal. Fluorescence signal from the antibody is in the left panel, and the corresponding transmitted light image is in the right panel. The XTH signal is specific to G-layers and is the strongest in the current growth ring (year 1) but it persists for 3 years. Note that only G-fibers (gf) are labeled, whereas normal fibers (nf), vessel elements (v) and ray cells (r), with the exception of contact ray cells, do not bind XET16A antibody. Bar = 25 μm; all photographs are taken at the same magnification.

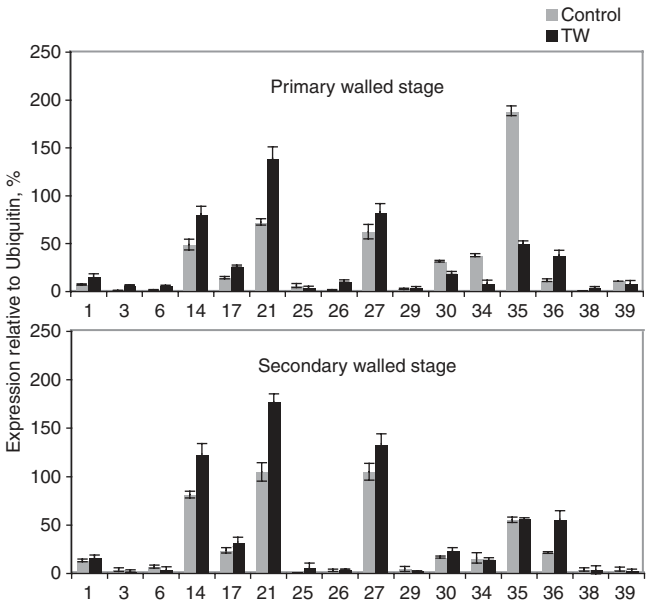

Fig. 7 Macroarray analysis of the XTH gene expression pattern in developing tension wood (TW) and normal wood (Control) at two developmental stages. Gene-specific 3′-untranslated regions were used to make a macroarray of wood-related *XTH* genes (designated by a number on the *x*-axis) and the signal from each *XTH* gene relative to the signal from polyubiquitin 4 was recorded. Results from triplicate hybridizations; error bar = SE.

XTH transcripts in developing TW compared with NW. However, these data need to be treated with caution as false-positive signals are probably due to the cross-hybridization of the highly expressed similar genes. Therefore, we designed a gene-specific macroarray for 16 wood-expressed *XTH* genes. *XTH* gene-specific cDNA fragments were spotted onto a nylon membrane along with three constitutively expressed unrelated genes that were used to calibrate the *XTH* gene expression levels. The macroarrays were hybridized to the cDNAs extracted from the developing TW and NW. Within each wood sample, two developmental stages were distinguished and hybridized separately: the early stage when cells had primary cell walls only (dividing and radially expanding cells) extracted from the phloem side; and the late stage when fibers were developing secondary walls including S_1, S_2 and the G-layer (Mellerowicz et al. 2001) that was extracted from the xylem side. After normalization of signals to the ubiquitin signals that did not vary between TW and NW, three *XTH* genes were highly expressed in developing TW at both primary and secondary walled stages. These were *XTH16-21*, *XTH16-14* and *XTH16-27* (Fig. 7). All three genes, but particularly *XTH16-21*, were up-regulated in TW compared with NW at both developmental stages. In addition, *XTH16-36* was up-regulated >2-fold in TW at both stages. In contrast, *XTH16-35* and *XTH16-34*, which are most highly and specifically expressed during the primary walled stage in NW, were the most down-regulated in TW. Interestingly, there was no overall change in the *XTH* gene expression at the primary walled stage between NW and TW although there were three genes that were expressed at very low levels in TW but were highly up-regulated (*XTH16-3*, *XTH16-6* and *XTH16-26*). In contrast, there was a general approximately 2-fold up-regulation of the gene family at the secondary walled stage due to the up-regulation of several highly expressed genes.

Discussion

The G-layer contains XG

Early studies in *P. tremula* of isolated G-layers using hydrolysis and paper chromatography found 98.5% of glucose and 1.5% of xylose in the layer (Norberg and Meier 1966). Therefore, it was assumed that the G-layer consists of almost pure cellulose, while the source of the xylose was not investigated further. Subsequently several authors reported small amounts of different compounds in this layer, such as pectin (Norberg and Meier 1966), hemicellulose (Furuya et al. 1970), β-1,4 galactan (E.J. Mellerowicz and T.A. Gorshkova, unpublished), arabinogalactan II (Lafarguette et al. 2004) and even lignin (Joseleau et al. 2004). These studies, however, deduced the composition of the layer either based on a chemical analysis of isolated layers or by in situ epitope labeling. Each of these approaches is prone to errors when detecting a substance present in low quantity. Consequently, the non-cellulosic components of the G-layers were not firmly established. In the present study, we provide evidence from a combined analysis: epitope labeling, in situ XET activity assay and neutral sugar and carbohydrate linkage analyses of isolated G-layers, all pointing to the presence of XG in the G-layers. Hydrolysis with sulfuric acid of the neutral sugars of isolated G-layers and analysis using the alditol acetate method and gas chromatography confirmed the presence of a small amount of xylose, galactose, mannose and arabinose observed earlier in *P. euroamericana* (Furuya et al. 1970), and also revealed the presence of fucose (Table 1), suggesting that XG is one of the most important additives in the G-layer. This hypothesis was confirmed conclusively by the linkage analysis that detected all the main XG components (Table 2). Based on the large amount of 4,6-linked glucose, it appears that XG is the most important non-cellulosic component of the layer and thus is unlikely to come from a contaminant of the isolated layers. This point was further demonstrated by two in situ labeling techniques in developing G-fibers. First, the monoclonal antibody CCRC-M1, a well-established marker for the fucosylated

side chain of XG (Puhlmann et al. 1994), detected a signal in the G-layer throughout its development (Fig. 2). The antibody is also known to label the fucose epitope in rhamnogalacturonan I (RGI). However, the abundance of RGI in the G-layer could be excluded based on the sugar composition analysis and linkage analysis. Secondly, the in situ XET activity assay that localizes both XET activity and the donor XG (Vissenberg et al. 2000) showed very strong signal in the developing G-layer (Figs. 3 and 4). Thus, the chemical, enzymological and immunohistochemical data indicate that the G-layer contains a small amount of XG, which is probably the most important non-cellulosic carbohydrate of the layer.

During maturation of G-fibers, the site of XXXG-SR incorporation shifts from the G-layer to the adjacent S_2-layer concomitant with the disappearance of CCRC-M1 signal from the G-layer. However, the chemical analysis shows that the XG is still present in the G-layer; the polysaccharide must therefore become inaccessible to large protein molecules. The mechanism of this phenomenon is not clear at present, although this developmental shift appears to be a part of the process of G-layer maturation. Interestingly, arabinogalactan-proteins, which are considered likely candidates for in vivo XET activity regulation (Takeda and Fry 2004), are spectacularly up-regulated during TW formation (Lafarguette et al. 2004, Andersson-Gunneråas et al. 2006). Perhaps FLA12-like proteins and XG interact in the wall, which might have implications for XET activity and XG accessibility.

The G-layer contains active XET

Immunolabeling of developing G-fibers with poplar XET16A polyclonal antibody revealed the presence of strong signals in the G-layer present in developing as well as in fully mature G-fibers. These signals were matched exactly, or were in close proximity to, the sites of incorporation of XXXG-SR that marks XET activity in the wall in the developing and mature G-fibers, respectively. In addition, transcripts of several GH16 *XTH* genes increased in developing secondary wall forming TW compared with NW, indicating that some *XTH* isoforms are induced during the formation of the G-layer. Thus, the combined evidence strongly indicates that the active XET enzyme acts in the developing G-layer. In this context, it is interesting to recall that a subfamily A alpha expansin *PttExpA5* was highly expressed and up-regulated in secondary wall forming TW compared with NW (Gray-Mitsumune et al. 2004, Andersson-Gunneråas et al. 2006). It is tempting to suggest that *Ptt*EXPA5 acts along with specific *XTH* gene products in remodeling of XG–cellulose frameworks of the G-layers rather than that of the primary walls.

Proposed role for XET in the G-fibers

Recent studies showed that cellulose microfibrils of the G-layer accumulate residual strain of the same order of magnitude as that observed in TW, pointing to the major role of cellulose microfibrils in generation of growth strains (Clair et al. 2006b). If the G-layer is to pull G-fibers to effect stem bending, its attachment of the outer cell wall layers is critical. This attachment is weak and is easily disrupted when the G-fiber is transversally cut (Clair et al. 2005). Therefore, XET activity might act to maintain the connections between G- and S_2-layers. If cellulose microfibrils shrink uniformly in all cell wall layers during maturation, the layers would shrink differentially because they have different microfibril angles (Araki et al. 1982, Prodhan et al. 1995), and they would move past each other, necessitating a cross-linking activity to repair cell wall integrity. XET activity could serve to repair the broken cross-links between the layers to keep them together. Thus, XET activity is proposed to be essential for the mechanism of stem bending. In agreement with this prediction, it has recently been shown experimentally that transgenic poplars that had a reduced XG content due to expression of a fungal xyloglucanase were not able to raise their stems from the leaning position (Kei'ichi Baba, Miyuki Takeuchi, Yong Woo Park, Machiko Sawada and T. Hayashi, in preparation).

We showed that several abundant *XTH* genes were generally up-regulated during TW formation, including *XTH16-36*, *-21*, *-14* and *-27*, while others were suppressed (*XTH16-35*). The transcriptome data also revealed that some XTH genes which were expressed at a low level were up-regulated specifically during primary wall formation in TW (e.g. *XTH16-26*). This suggests specialized functions of these XTHs genes. Interestingly, the proteome analysis of developing TW identified the *XTH16-26* gene product as highly abundant (Kei'ichi Baba, Miyuki Takeuchi, Yong Woo Park, Machiko Sawada and T. Hayashi, in preparation) even though its transcript was not abundant in our analysis.

To date, the activity of approximately 10 *XTH* gene products has been rigorously correlated with their primary sequence by heterologous expression and quantitative kinetic analysis. Of these, all but one have been shown to have predominantly or uniquely XET activity. NXG1 from *Tropaeolum majus* (nasturtium) is the exception; this enzyme is a predominant *endo*-xyloglucanase [xyloglucan *endo*-hydrolase (XEH) EC 3.2.1.151] (Edwards et al. 1986, de Silva et al. 1993, Fanutti et al. 1993, Chanliaud et al. 2004). The three-dimensional structures of *Ptt*XET16A and more recently also NXG1 have been solved and used along with quantitative kinetic assays to perform structure–function comparison of these enzyme archetypes (Johansson et al. 2004, Kallas et al. 2005,

Baumann et al. 2007). Subsequent structure-based phylogenetic analysis using a maximum likelihood method and approximately 130 plant whole-genome and EST sequences has clearly indicated that the traditional classification of *XTH* gene products into three or four major subgroups (Campbell and Braam 1999a, Yokoyama et al. 2004) has limited value with respect to functional prediction (Saladié et al. 2006, Baumann et al. 2007). Indeed, bootstrap values indicated that the traditional subgroups are not statistically robust, and that there may be a greater number of stable phylogenetic clades. Catalytic diversity within all of these clades has not yet been cataloged. We note, however, that in TW, no transcripts of *Populus* homologs were observed which cluster in the NXG1 clade (*Ptt*XTH16-7, *Ptt*XTH16-31 and *Ptt*XTH16-32). Hydrolytic (*endo*-xyloglucanase) activity has not yet been found outside of this clade composed of nine of approximately 100 *Arabidopsis thaliana*, *Oryza sativa* and *Populus trichocarpa XTH* genomic sequences. Therefore, we cautiously predict that the TW *XTH* transcripts observed in the present study encode XETs that participate in cross-link repair during G-fiber development, essential for shrinking of the fiber.

In a likely scenario, XETs of the G-layer are active in transglycosylation first in the developing layer and later at the interface between S_2- and G-layers in the fully mature G-fibers. Since XG has not been previously demonstrated in S_1/S_2 wall layers, it is possible that the transglycosylation activity in these layers involves a different polysaccharide donor substrate (Mohad and Farkaš 2006), or a transglycosylase from another CAZy family, which is capable of using xylo-oligosaccharides as acceptor substrates. To investigate the possibility of donor promiscuity further, detailed enzymatic characterization of heterologously expressed GH16 *XTH* genes (Kallas et al. 2005) up-regulated during TW formation will be required.

XET in G-fibers may be active beyond the fiber lifespan

The finding of *XTH* gene product and demonstration of XET activity in the G-fibers that were several years old indicates that the enzyme might be active in these fibers beyond the lifespan of their protoplasts. Such activity is theoretically possible as the substrates for the transglycosylation reaction are already present in the wall. One can imagine that the unequal shrinking of the cell wall layers might continue for several years in G-fibers, for example as a result of moisture changes. XET activity would then help to maintain the mechanical integrity of the G-fiber wall helping the TW tissue to perform its function. Both *XTH* gene product and XET activity persist in the mature G-fibers specifically and are absent in the NW fibers, which indicates that such post-mortem activity is not normally required for tissue integrity in NW. There are several examples of cells in plant tissues which function after cell death. Vessel elements, aerenchyma, epidermal hairs involved in seed dispersal, and cells forming different catapulting devices of dry fruits are some of the examples. TW fibers would appear to form yet another category of cells functioning after death in which the enzymatic activity is continued.

Materials and Methods

Plant material

Most work was done using the hybrid aspen *P. tremula* L. × *tremuloides* Michx. trees grown in the greenhouse under natural light conditions supplemented with metal halogen lamps with an 18 h light/6 h dark photoperiod at a temperature of 22°C/15°C (day/night). They were watered daily and fertilized once a week with a SuperbraS nutrient solution (Supra Hydro AB, Landskrona, Sweden). TW was induced by leaning the trees at about a 45° angle in the greenhouse for 19 d. In some experiments, older material was used from outdoor-grown trees of *P. tremula* and *P. alba*. Either leaning stems or branches were used as a source of TW.

Isolation of the G-layer

Branches of poplar trees (*P. alba*), about 5–10 cm in diameter, were collected and stored in 96% ethanol. Isolation of the G-layer from transverse sections of TW was performed according to Norberg and Meier (1966). Wood blocks from a branch were treated with a zinc-chloro-iodide solution to stain G-layers. Transverse sections 20 µm thick were prepared from the TW areas with a sliding-microtome. The sections were incubated in 96% ethanol for a few hours in order to shrink the G-layers, thus loosening them from the S_2-layers, and treated for 30 min with ultrasonic waves (Yamato Branson 1210). G-layers shaken out of the sections were separated from the sections with a 1G2 glass filter (pore size ~50 µm). The purity of the isolated G-layer fraction was confirmed by microscopic observation (Fig. 1).

Neutral sugar analysis

The neutral sugar composition of the isolated G-layer was determined by the alditol acetate method with minor modification (Borchardt and Piper 1970). The isolated G-layer (7.8 mg) was hydrolyzed with 0.3 ml of 72% sulfuric acid for 1 h at 30°C, diluted with 8.4 ml of water and autoclaved for 1 h at 120°C to hydrolyze cell wall polysaccharides completely. After cooling the hydrolysate, 10 mg of *myo*-inositol was added as an internal standard. The solution was neutralized with a saturated solution of barium hydroxide to a pH of 5.5, and centrifuged for 15 min at 3,000 × *g*. A 2 ml aliquot of the supernatant was transferred to a round bottom flask (50 ml). Then 20 mg of sodium borohydride were added to the flask, mixed and allowed to react overnight at room temperature. To decompose the excess borohydride, acetic acid was added until gas evolution ceased. The solution was concentrated to a syrup with a rotary evaporator (60°C). To remove the volatile methyl borate esters, 10 ml of ethanol was added to the syrup and evaporated to dryness three times. The alditols were dried in an oven at 105°C for 15 min to insure complete removal of water. The mixture of 0.1 ml of concentrated sulfuric acid and 2 ml of acetic anhydride was added to the flask and allowed to react for 1 h at 60°C. The flask was removed from the water bath and cooled for 5 min. The reaction mixture was transferred slowly into 20 ml of water with stirring. The mixture was transferred to a separating

funnel, and the alditol acetates were extracted with 15 ml of ethyl acetate. A 20 ml aliquot of saturated sodium hydrogen carbonate was added to the organic phase and then the water phase was discarded. The organic phase was washed with 20 ml of distilled water. A second 20 ml aliquot of saturated sodium chloride was added to the organic phase and then the water phase was discarded. The organic phase was completely dehydrated by passing through a column containing sodium sulfate. The extracts were concentrated to near dryness with the rotary evaporator (60°C). The residue (alditol acetates) was dissolved in 1 ml of acetone. The alditol acetates were quantitatively determined by gas chromatography on a fused silica capillary column (SP-2330, 0.25 mm × 15 m, SPELCO, Bellefonte, PA, USA).

Methylation analysis

The isolated G-layers (4.1 mg) were completely dissolved in 1 ml of DMSO containing 0.15 g of tetrabutylammonium fluoride (Lu and Ralph 2003). The dissolved sample was subjected to methylation analysis (Hakomori 1964). Partially methylated alditol acetates were analyzed by gas chromatography on a glass capillary column (0.25 × 15 m) of DB-225.

Table 3 Gene-specific primer pairs used for macroarray spots

Gene	Former gene name	GenBank accession No.	Forward primer/reverse primer (5′ to 3′)
XTH16-34	*XET16A*	AF515607	AGTTCCAAGATCTGGATGCCTTC
			TGGTTCATTACAGTTTGACAACA
XTH16-26	*XET16B*	EF194046	TTCATAGCCTCCTACAAGAGCTTCC
			TTATTAAACAGAAGTGACCCGTCCA
XTH16-35	*XET16C*	EF151160	TGCATACCAATATGGAAAACAAAGG
			ATGGAGGACATGTTTATCTGGCTTT
XTH16-36	*XET16D*	EF194050	ACGCCATGGAAGCTAGGAAATATAG
			GCGCACAATAATAGACGAGCTTTT
XTH16-6	*XET16E*	EF194049	GCCAACCAATGTGGATATACTCAAG
			CATTTTATTGGTGGAGATTCAAGAAA
XTH16-21	*XET16G*	EF194058	ACGAAGGCACCCTTTACAGCTTACT
			ATCAACAACACGAAAAGGGTAGGTAA
XTH16-30	*XET16H*	EF194057	CGATAGCAGCAGATGATAACGCTAA
			TTTGCTCAGTGAGGCCATTGTTAC
XTH16-17	*XET16I*	EF194056	GAGTCTATGGAATGCTGATGACTGG
			TGGGAATCTTTCTTTTACTTTCATCG
XTH16-39	*XET16J*	EF194055	AAGGTTCCTCCATCAGAGTGTGTAA
			GCGAGGGTGTCAAAATAGTACAGAA
XTH16-14	*XET16K*	EF194054	ACTTGGTCTTACGGTGCTTCTTCTT
			AACAAGATTCTTTATTATCTGGAGAACG
XTH16-3	*XET16M*	EF194053	GATTTCGCCAACGTTACATGTATTA
			TATTCTGGCATTGATCAAGCGTACT
XTH16-27	*XET16R*	EF194052	TCCTACAAGAGCTTCCACATAGACG
			CAAGCCGAGAGTAATAACGAAAACA
XTH16-1	*XET16S*	EF194048	ACAAGAACAATGGAGAACCAAACAG
			CCCATCTCAAAATGATATCCAAGAA
XTH16-38	*XET16T*	EF194047	CACAGCAGTTCTTACCCTTCTGTGT
			GGAGGAAACATTGGTTTGTGTTTCT
XTH16-25	*XET16AA*	EF194051	TAAAGTTCCAGTAAGGGTGCACAAG
			TTGTGATTTATACCCATCTCAAAACG
XTH16-29	*XET16BB*	EF194045	TTCCATACTTATTCGGTCTTGTGGA
			CATTCTTTTGGGAGGTTATTTTGGA
ADF6			CTTTGACTTCGTGACGTCTGAGAAT
			ATTGCCAAGTATCCACCAACTTACA
ELF4A			ACACAGTCTCAGCTACTCATGGTGA
			TCATGCTGTAATAATGAAGGGAGGA
UBQ4			AGGACACTTGCTGACTACAACATCC
			TGCTTAAATACGAAAGCTTCCAATG

Immunolocalization

Immunolabeling of sections of poplar wood-forming tissues was as described by Bourquin et al. (2002). The polyclonal antibody XET16A was raised against heterologously expressed *Ptt*XET16-34 protein without the signal peptide (Bourquin et al. 2002). The background antibody staining was verified by using a pre-immune serum instead of the antibody at the same immunoglobin concentration. CCRC-M1 monoclonal antibody was a gift from Dr. M. Hahn. The background fluorescence was evaluated with a negative control where the primary antibody was omitted. The secondary antibodies used were conjugated to either fluorescein isothiocyanate (FITC) or Alexa-488. Sections were examined using a Zeiss LM510 confocal microscope using the argon–krypton laser at 488 nm. The FITC and Alexa 488 signal was detected between 505 and 530 nm. All fluorescence detection settings were kept at the same level for the sets of samples being compared.

In situ XET activity localization

The procedures for in situ XET activity detection were based on Vissenberg et al. (2000) with modifications (Bourquin et al. 2002), except that the monocomponent substrate XXXG-SR was used in place of an XGO-SR mixture. Briefly, XXXG-SR was synthesized from XXXG-NH_2 (Greffe et al. 2005) according to the method devised by Fry (1997), except that dimethylformamide was used as the solvent. The product was precipitated from the reaction mixture using 10 vols. of 2-propanol and dissolved in a minimal amount of water (0.5 ml). The precipitation was repeated twice to remove excess unreacted sulforhodamine chloride. The resulting crude material was dissolved in water (1 ml) and purified on an RP-18 cartridge (5 ml) using a step-wise gradient of acetonitrile in water (0–25%, product eluted at ~7–10%). The product gave a satisfactory ESI-TOF (electrospray ionization-time of flight) mass spectrum (Eneyskaya et al. 2005): $[M+2Na]_{2+}$ calculated m/z 824.749, observed 824.708.

Sections with labeled reaction products were examined using a Zeiss LM510 confocal microscope. All fluorescence detection settings were kept at the same level for the sets of samples being compared. Autofluorescence of the tissues was verified before each experiment. Sections boiled for 10 min were always used as negative controls.

Macroarray for the analysis of XTH gene expression

For the macroarray analysis, we used 16 poplar *XTH* genes that are related to wood formation. Gene names and the GenBank accession numbers are listed in Table 3. Gene-specific fragments of 400–500 bp from the 3′-untranslated sequences were amplified by PCR with the gene-specific primers (Table 3) using 11 full-length cDNA clones from the EST library and five cDNA fragments from reverse transcription–PCR (RT–PCR) as templates. A 100 ng aliquot of purified PCR product of each gene fragment was dot spotted onto a HybondN nylon membrane (Amersham Pharmacia Biotech, Uppsala, Sweden). Three genes were selected as positive controls, actin-depolymerizing factor 6 (N010G05; ADF6), eukaryotic initiation factor 4A-8 (UK118TF08; eIF4A-8) and polyubiquitin 4 (N022H08; UBQ4), based on their constitutive expression in the different tissues of poplar.

Stem segments were frozen in liquid nitrogen. For RNA extraction, the segments were thawed to allow bark peeling, and the exposed developing wood surfaces were scraped with a scalpel to isolate primary walled and secondary walled developing xylem (Gray-Mitsumune et al. 2004). Care was taken to avoid as much as possible phloem contamination when scraping the bark side. The tissue was ground in liquid nitrogen. The mRNA was directly extracted from frozen tissue powder using paramagnetic oligo(dT)25 Dynabeads (Dynal AS, Norway) according to the manufacturer's instructions. The cDNA was labeled with ^{32}P by a reverse transcription reaction with specific primer mixtures for each target *XTH* and the control genes. Two independent trees were tested and the hybridizations were repeated three times.

Acknowledgments

This work was supported by grants to E.J.M. from Formas, Swedish Research Council, Wallenberg Foundation, European project Eden QLK5-CT-2001-00443, Wood Ultrastructure Research Centre and UPSC Plant Development Excellence Centre. Substrate synthesis at KTH Biotechnology was supported by a grant from the Swedish Foundation for Strategic Research (SSF). H.B. is a Fellow of the Swedish Research Council.

References

Almeras, T., Thibaut, A. and Gril, J. (2005) Effect of circumferential heterogeneity of wood maturation strain, modulus of elasticity and radial growth on the regulation of stem orientation in trees. *Trees—Struct. Funct*. 19: 457–467.

Andersson-Gunnerås, S., Mellerowicz, E.J., Love, J., Segerman, B., Ohmiya, Y., Coutinho, P.M., Nilsson, P., Henrissat, B., Moritz, T. and Sundberg, B. (2006) Making cellulose enriched tension wood in *Populus*: global analysis of transcripts and metabolites identifies biochemical and developmental regulators in secondary wall biosynthesis. *Plant J*. 45: 144–165.

Araki, N., Fujita, M., Saiki, H. and Harada, H. (1982) Transition of the fiber wall structure from normal wood to tension wood in *Robinia pseudoacacia* L. and *Populus euroamericana* Guinier. *Mokuzai Gakkaishi* 28: 267–273.

Bamber, R.K. (2001) A general theory for the origin of growth stresses in reaction wood: how trees stay upright. *IAWA J*. 22: 205–212.

Baumann, M.J., Eklöf, J.M., Michel, G., Kallas, Å.M., Teeri, T.T., Czjzek, M. and Brumer, H., III (2007) Structural evidence for the evolution of xyloglucanase activity from XETs: biological implications for cell wall metabolism. *Plant Cell*, in press.

Borchardt, L.G. and Piper, C.V. (1970) A gas chromatographic method for carbohydrates as alditol-acetates. *TAPPI* 53: 257–260.

Bourquin, V., Nishikubo, N., Abe, H., Brumer, H., Denman, S., Eklund, M., Christiernin, M., Teeri, T.T., Sundberg, B. and Mellerowicz, E.J. (2002) Xyloglucan endotransglycosylases have a function during the formation of secondary cell walls of vascular tissues. *Plant Cell* 14: 3073–3088.

Campbell, P. and Braam, J. (1999) Xyloglucan endotransglycosylases: diversity of genes, enzymes and potential wall-modifying functions. *Trends Plant Sci*. 4: 361–366.

Chanliaud, E., de Silva, J., Strongitharm, B., Jeronimidis, G. and Gidley, M.J. (2004) Mechanical effects of plant cell wall enzymes on cellulose/xyloglucan composites. *Plant J*. 38: 27–37.

Clair, B., Almeras, T. and Sugiyama, J. (2006a) Compression stress in opposite wood of angiosperms: observations in chestnut, mani and poplar. *Ann. Forest Sci*. 63: 507–510.

Clair, B., Almeras, T., Yamamoto, H., Okuyama, T. and Sugiyama, J. (2006b) Mechanical behavior of cellulose microfibrils in tension wood, in relation with maturation stress generation. *Biophys. J*. 91: 1128–1135.

Clair, B., Ruelle, J., Beauchene, J., Prevost, M.F. and Fournier, M. (2006c) Tension wood and opposite wood in 21 tropical rain forest species 1. Occurrence and efficiency of the G-layer. *IAWA J*. 27: 329–338.

Clair, B., Thibaut, B. and Sugiyama, J. (2005) On the detachment of the gelatinous layer in tension wood fiber. *J. Wood Sci*. 51: 218–221.

Edwards, M., Dea, I.C.M., Bulpin, P.V. and Reid, J.S.G. (1986) Purification and properties of a novel xyloglucan-specific endo-(1–4)-beta-D-glucanase from germinated nasturtium seeds (*Tropaeolum-majus* L). *J. Biol. Chem.* 261: 9489–9494.

Eneyskaya, E.V., Ivanen, D.R., Shabalin, K.A., Kulminskaya, A.A., Backinowsky, L.V., Brumer, H. and Neustroev, K.N. (2005) Chemo-enzymatic synthesis of 4-methylumbelliferyl beta (1–4)-D-xylooligosides: new substrates for beta-D-xylanase assays. *Org. Biomol. Chem.* 3: 146–151.

de Silva, J., Jarman, C.D., Arrowsmith, D.A., Stronach, M.S., Chengappa, S., Sidebottom, C. and Reid, J.S.G. (1993) Molecular characterization of a xyloglucan-specific endo-(1–4)-beta-D-glucanase (xyloglucan endotransglycosylase) from nasturtium seeds. *Plant J.* 3: 701–711.

Fanutti, C., Gidley, M.J. and Reid, J.S.G. (1993) Action of a pure xyloglucan endo-transglycosylase (formerly called xyloglucan-specific endo-(1–4)-beta-D-glucanase) from the cotyledons of germinated nasturtium seeds. *Plant J.* 3: 691–700.

Fournier, M., Chanson, B., Thibaut, B. and Guitard, D. (1994) Measurements of residual growth strains at the stem surface: observations on different species. *Ann. Sci. Forest.* 51: 249–266.

Fry, S.C. (1997) Novel 'dot-blot' assays for glycosyltransferases and glycosylhydrolases: optimization for xyloglucan endotransglycosylase (XET) activity. *Plant J.* 11: 1141–1150.

Furuya, S., Takahashi, and Miyazaki, M. (1970) The chemical composition of gelatinous layer from the tension wood of *Populus euro-americana*. *J. Jpn Wood Res. Soc.* 16: 26–30.

Geisler-Lee, J., Geisler, M., Coutinho, P.M., Segerman, B., Nishikubo, N., et al. (2006) Poplar carbohydrate-active enzymes (CAZymes). Gene identification and expression analyses. *Plant Physiol.* 140: 1–17.

Gray-Mitsumune, M., Mellerowicz, E.J., Abe, H., McQueen-Mason, S., Winzéll, A., Sterky, F., Blomqvist, K., Schrader, J., Teeri, T.T. and Sundberg, B. (2004) .Expansins abundant in secondary xylem belong to subgroup A of the α-expansin gene family. *Plant Physiol.* 135: 1552–1564.

Greffe, L., Bessueille, L., Bulone, V. and Brumer, H. (2005) Synthesis, preliminary characterization, and application of novel surfactants from highly branched xyloglucan oligosaccharides. *Glycobiology* 15: 437–445.

Hakomori, S. (1964) A rapid permethylation of glycolipid and polysaccharide catalyzed by methylsulfinyl carbanion in dimethyl sulfoxide. *J. Biochem.* 55: 205–208.

Hejnowicz, Z. (1997) Graviresponses in herbs and trees: a major role for the redistribution of tissue and growth stresses. *Planta* 203: S136–S146.

Johansson, P., Brumer, H., Baumann, M.J., Kallas, Å.M., Henriksson, H., Denman, S.E., Teeri, T.T. and Jones, T.A. (2004) Crystal structures of a poplar xyloglucan endotransglycosylase reveal details of transglycosylation acceptor binding. *Plant Cell* 16: 874–886.

Joseleau, J.P., Imai, T., Kuroda, K. and Ruel, K. (2004) Detection in situ and characterization of lignin in the G-layer of tension wood fibres of *Populus deltoides*. *Planta* 219: 338–345.

Kallas, Å.M., Piens, K., Denman, S., Henriksson, H., Fäldt, J., Johansson, P., Brumer, H. and Teeri, T.T. (2005) Enzymatic properties of native and deglycosylated hybrid aspen (*Populus tremula* × *tremuloides*) xyloglucan endotransglycosylase 16A expressed in *Pichia pastoris*. *Biochem. J.* 390: 105–113.

Lafarguette, F., Leple, J.C., Dejardin, A., Laurans, F., Costa, G., Lesage-Descauses, M.C. and Pilate, G. (2004) Poplar genes encoding fasciclin-like arabinogalactan proteins are highly expressed in tension wood. *New Phytol.* 164: 107–121.

Lu, F. and Ralph, J. (2003) Non-degradative dissolution and acetylation of ball-milled plant cell walls: high-resolution solution-state NMR. *Plant J.* 35: 535–544.

Mellerowicz, E.J., Baucher, M., Sundberg, B. and Boerjan, W. (2001) Unravelling cell wall formation in the woody dicot stem. *Plant Mol. Biol.* 47: 239–274.

Mohand, F.A. and Farkaš, V. (2006) Screening for hetero-transglycosylating activities in extracts from nasturtium (*Tropaeolum majus*). *Carbohydr. Res.* 341: 577–581.

Norberg, H. and Meier, H. (1966) Physical and chemical properties of the gelatinous layer in tension wood fiber of Aspen (*Populus tremula* L.). *Holzforschung* 20: 174–178.

Pilate, G., Dejardin, A., Laurans, F. and Leple, J.C. (2004) Tension wood as a model for functional genomics of wood formation. *New Phytol.* 164: 63–72.

Plomion, C., Leprovost, G. and Stokes, A. (2001) Wood formation in trees. *Plant Physiol.* 127: 1513–1523.

Prodhan, A.K.M.A, Funada, R., Ohtani, J., Abe, H. and Fukazawa, K. (1995) Orientation of microfibrils and microtubules in developing tension-wood fibres of Japanese ash (*Fraxinus mandshurica* var. *japonica*). *Planta* 196: 577–585.

Puhlmann, J., Bucheli, E., Swain, M.J., Dunning, N., Albersheim, P., Darvill, A.G. and Hahn, M.G. (1994) Generation of monoclonal antibodies against plant cell wall polysaccharides. I. Characterization of a monoclonal antibody to a terminal α-(1→2)-linked fucosyl-containing epitope. *Plant Physiol.* 104: 699–710.

Saladié, M, Rose, J.K.C., Cosgrove, D.J. and Catala, C. (2006) Characterization of a new xyloglucan endotransglucosylase/hydrolase (XTH) from ripening tomato fruit and implications for the diverse modes of enzymic action. *Plant J.* 47: 282–295.

Takeda, T. and Fry, S.C. (2004) Control of xyloglucan endotransglucosylase activity by salts and anionic polymers. *Planta* 219: 722–732.

Timell, T.E. (1986) Compression Wood in Gymnosperms Vol. 2. pp. 983–1262. Springer-Verlag, Heidelberg.

Vissenberg, K., Martinez-Vilchez, I.M., Verbelen, J.-P., Miller, J.G. and Fry, S.C. (2000) In vivo colocalization of xyloglucan endotransglycosylase activity and its donor substrate in the elongation zone of Arabidopsis roots. *Plant Cell* 12: 1229–1238.

Yamamoto, H., Abe, K., Arakawa, Y., Okuyama, T. and Gril, J. (2005) Role of the gelatinous layer (G-layer) on the origin of the physical properties of the tension wood of *Acer sieboldianum*. *J. Wood Sci.* 51: 222–233.

Yokoyama, R., Rose, J.K.C. and Nishitani, K. (2004) A surprising diversity and abundance of xyloglucan endotransglucosylase/hydrolases in rice. Classification and expression analysis. *Plant Physiol.* 134: 1088–1099.

(Received March 1, 2007; Accepted May 8, 2007)